Magnetic Susceptibility Artifacts in Magnetic Resonance Imaging: Calculation of the Magnetic Field Disturbances

Stéphane Balac and Gabriel Caloz
Institut de Recherche Mathématique de Rennes, U.R.A. C.N.R.S. 305,
Université de Rennes 1, F-35042 Rennes, France

Abstract— **In Magnetic Resonance Imaging, inhomogeneities of the static magnetic field lead to perturbations in the resulting images, called artifacts. Our goal is to numerically compute the disturbances induced by a material having magnetic properties different from that of the surrounding tissues (e.g. a paramagnetic implant). Since the method is linked to an artifact reconstruction model to get simulated images, it has to be well suited for general three dimensional geometries and to provide very accurate results in a fine grid around the implant. Our method is based on a surface integral representation of the magnetic field. An analytical expression is derived when the boundary of the domain can be meshed in flat panels. For curved surfaces a numerical quadrature scheme is implemented.**

I. Introduction

In a Magnetic Resonance Imaging (MRI) device [1], a sample lies in a highly homogeneous static magnetic field $\overrightarrow{B_0}$. One of the most common measuring protocol is the spin-echo spin-warp one. In this protocol, the nuclear spins are excited by a 90^o RF pulse and refocused by a 180^o pulse. The resulting RF signal is collected. The spatial localization is achieved by applying magnetic field gradients along three space directions. A slice of the object is selected with the help of a gradient – the slice selection gradient – which is switched on during RF pulses. An image of this slice is obtained with the aid of a further gradient: the phase-encoding gradient just after the excitation pulse and the read-out gradient during data collection. The procedure is repeated when varying the strength of the phase encoding gradient. Finally the image is reconstructed through the two-dimensional Fourier transform of the collected data.

If the sample contains an object having a magnetic susceptibility different from that of the tissue, then an additional magnetic field appears. The static field is not homogeneous any longer and artifacts will appear in the images.

Manuscript received July 10, 1995.

S. Balac, e-mail balac@lie.univ-rennes1.fr; G. Caloz, e-mail caloz@lie.univ-rennes1.fr.

This works is carried out within the framework of the research group *G.I.S. biomatériaux métalliques* at the University of Rennes.

The principles governing the resulting changes in the image have been analysed, see for instance [2]–[4]. A point in the sample where the static field differs from the expected one will have, in the imaging process, the properties expected from another point, shifted in the directions of the slice selection and the read-out gradients.

Previous works [5], [3] have studied artefacts generated by a metallic ball, for which an analytical expression for the induced magnetic field is known. We propose a computational procedure to calculate the magnetic field induced by a paramagnetic body of a quite general geometry. The method is based on a surface integral representation of the magnetic field.

An analytical expression is derived when the boundary of the domain can be partitioned into a set of flat panels. For curved domains, a meshing of the surface as a collection of flat triangles is generally not efficient and to get the desired accuracy the use of curved triangles is required. Then analytical expressions cannot be obtained and a numerical quadrature rule is needed. These two methods are implemented altogether so that when the boundary is formed of a set of both flat and curved panels the best suited method can be used.

II. Computation of Magnetic Field Disturbances

A. Mathematical Modelling

Let us consider an object Ω (Ω is an open bounded set in $\mathbb{R}^3$ with boundary Σ) having magnetic properties different from that of the surrounding tissue $\Omega' = \mathbb{R}^3 \backslash \bar{\Omega}$, assumed to be an homogeneous medium and placed in an MRI device. Ω is assumed to be an isotropic linear magnetic material. The exciting RF pulses are neglected.

Given an applied static magnetic field $\overrightarrow{B_0}$ we are concerned with finding the magnetic field induced by Ω. Since the metallic body is assumed to be paramagnetic, the induced field is very small compared to $\overrightarrow{B_0}$ and we will consider the magnetization being uniform in Ω. Moreover we assume that the magnetization of the outward domain can be neglected.

The basic equations for magnetostatics deduced from Maxwell equations lead to the problem: find $\overrightarrow{H}$ such that

$$\operatorname{div} \overrightarrow{H} = 0 \text{ in } \Omega \text{ and } \Omega', \tag{1}$$

$$\begin{aligned} \operatorname{curl} \overrightarrow{H} &= 0 \text{ in } \mathbb{R}^3, & (2)\\ \left[\overrightarrow{H}\cdot\overrightarrow{n}\right] &= -\overrightarrow{M}\cdot\overrightarrow{n} \text{ at the interface } \Sigma, & (3)\end{aligned}$$

where $\overrightarrow{n}$ the unit outward normal to Σ and $[\cdot]$ the jump across the boundary. $\overrightarrow{M}$ denotes the magnetization in the domain Ω.
At infinity $\overrightarrow{H}$ satisfies

$$\lim_{\substack{|x|\to\infty \\ x\in\mathbb{R}^3}} \overrightarrow{H}(x) = 0. \quad (4)$$

Problem (1)–(4) is the classical magnetostatic problem due to a surface current and is studied from a mathematical point of view in [7].

From equation (2) we can introduce the scalar magnetic potential Φ as unknown, $\overrightarrow{H} = -\nabla\Phi$. The potential Φ satisfies

$$\begin{aligned} \Delta\Phi &= 0 \text{ in } \Omega \text{ and } \Omega', & (5)\\ \left[\nabla\Phi\cdot\overrightarrow{n}\right] &= \overrightarrow{M}\cdot\overrightarrow{n} \text{ at the interface } \Sigma, & (6)\\ \Phi(x) &\longrightarrow 0 \text{ when } |x|\longrightarrow\infty. & (7)\end{aligned}$$

As is well known, the potential Φ can be represented by the integral formula

$$\Phi(P) = \frac{1}{4\pi}\iiint_\Omega \overrightarrow{M}\cdot\nabla_Q\frac{1}{|P-Q|}\mathrm{d}v(Q)\ . \quad (8)$$

The quantity of interest in the artefact reconstruction method is the flux density $\overrightarrow{B} = \mu\overrightarrow{H} = -\mu\nabla\Phi$. We have

$$\overrightarrow{B}(P) = -\frac{\mu}{4\pi}\nabla_P\iiint_\Omega \frac{\overrightarrow{M}\cdot\overrightarrow{r}}{r^3}\mathrm{d}v(Q)\ . \quad (9)$$

where $\overrightarrow{r} = \overrightarrow{QP}$.

Using the assumption that the magnetization $\overrightarrow{M}$ was uniform in Ω and the Gauss theorem, $\overrightarrow{B}$ defined by (9) can be rewritten in the form

$$\overrightarrow{B}(P) = \frac{\mu}{4\pi}\iint_\Sigma\left(\frac{\overrightarrow{M}\cdot\overrightarrow{r}}{r^3}\right)\overrightarrow{n}(Q)\ \mathrm{d}s(Q). \quad (10)$$

The numerical computation of $\overrightarrow{B}$ is discussed below.

B. Computational Method

We assume that the boundary Σ is meshed in a finite union of flat and curved triangles. Let T_h^1 denote the set of all flat triangles and T_h^2 the set of all curved triangles. (One of these sets can be empty.) We get

$$\Sigma = \bigcup_{K\in T_h^1} K \ \cup \bigcup_{K\in T_h^2} K\ .$$

We decompose $\overrightarrow{B}$ as given by (10) in two terms

$$\begin{aligned}\overrightarrow{B}(P) = &\frac{\mu}{4\pi}\sum_{K\in T_h^1}\iint_K \overrightarrow{M}\cdot\frac{\overrightarrow{r}(P,Q)}{r^3(P,Q)}\ \overrightarrow{n}(Q)\ \mathrm{d}s(Q)\\ &+\frac{\mu}{4\pi}\sum_{K\in T_h^2}\iint_K \overrightarrow{M}\cdot\frac{\overrightarrow{r}(P,Q)}{r^3(P,Q)}\ \overrightarrow{n}(Q)\ \mathrm{d}s(Q)\ . \quad (11)\end{aligned}$$

These two sums are evaluated using two distinct methods.

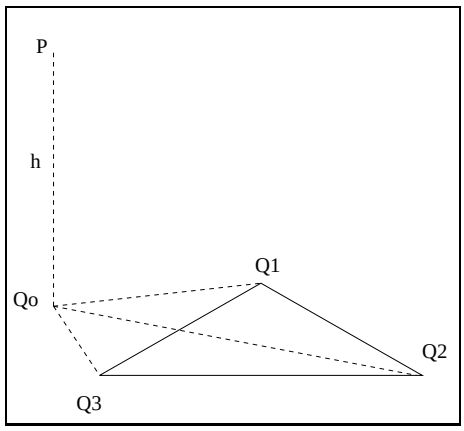

Fig. 1. Decomposition of triangle K.

C. Integration over flat triangles

Throughout this section we are concerned with the calculation of the first sum in (11), denoted S_1 . Since the triangles are flat, the normal $\overrightarrow{n}$ to Σ is constant on each triangle K (it will be denoted $\overrightarrow{n}_K$ in the sequel). Since the magnetization $\overrightarrow{M}$ is uniform on Ω we get

$$S_1(P) = \frac{\mu}{4\pi}\sum_{K\in T_h^1}\left(\overrightarrow{M}\cdot\iint_K\frac{\overrightarrow{r}(P,Q)}{r^3(P,Q)}\ \mathrm{d}s(Q)\right)\ \overrightarrow{n}_K\ . \quad (12)$$

An analytical expression over a triangle domain has been derived for the potential due to a uniform source distribution in [8]. Our technique used for calculating the field $\overrightarrow{B}$ is rather different.

Consider a triangle K having his vertices at the points Q_1, Q_2, Q_3. Let Q_0 be the projection of the point P on the plane defined by K. We introduce the following triangles: $K_1 = \{Q_0, Q_1, Q_2\}, K_2 = \{Q_0, Q_2, Q_3\}, K_3 = \{Q_0, Q_3, Q_1\}$, see Fig. 1.

We can decompose the integral over K in a sum of three integrals over K_1, K_2, K_3,

$$\iint_K\frac{\overrightarrow{r}}{r^3}\mathrm{d}s = \overset{+}{-}\iint_{K_1}\frac{\overrightarrow{r}}{r^3}\mathrm{d}s\overset{+}{-}\iint_{K_2}\frac{\overrightarrow{r}}{r^3}\mathrm{d}s\overset{+}{-}\iint_{K_3}\frac{\overrightarrow{r}}{r^3}\mathrm{d}s\ . \quad (13)$$

The sign to be taken into account for each of the three integrals can be easily obtained by computing the area co-ordinates of the triangle K for the point Q_0. (For instance, in the situation drawn in Fig. 1, the signs are $+, +$ and $-$.)

Let us consider the ith integral. For convenience of simplicity we will denote by $\{Q_0, Q_i, Q_j\}$ the vertices of the triangle K_i. We first introduce a new coordinate system with origin Q_0 and orthogonal basis vectors

$$\begin{cases} \overrightarrow{x} &= \overrightarrow{Q_0Q_i}\ /\ |\overrightarrow{Q_0Q_i}|\\ \overrightarrow{z} &= (\overrightarrow{Q_0Q_i}\wedge\overrightarrow{Q_0Q_j})\ /\ |\overrightarrow{Q_0Q_i}\wedge\overrightarrow{Q_0Q_j}|\\ \overrightarrow{y} &= \overrightarrow{z}\wedge\overrightarrow{x}\end{cases}$$

In this coordinate system the vertices are defined by: $Q_0 : (0,0)$, $Q_i : (x_i, 0)$ with $x_i \geq 0$, $Q_j : (x_j, y_j)$ with $y_j \geq 0$.

Let (x, y) be the coordinates of Q and $h = \overrightarrow{Q_0P} \cdot \overrightarrow{z}$, then $\overrightarrow{r} = \overrightarrow{QP} = -x\ \overrightarrow{x} - y\ \overrightarrow{y} + h\ \overrightarrow{z}$.

The coordinates of the vector valued integral $\overrightarrow{R} = \iint_{K_i} \frac{\overrightarrow{r}}{r^3} \mathrm{d}s$, are

$$\begin{aligned} R_1 &= \iint_{K_i} \frac{-x}{(x^2+y^2+h^2)^{3/2}} \mathrm{d}x\mathrm{d}y \\ &= \iint_{K_i} \frac{\partial}{\partial x} \frac{1}{\sqrt{x^2+y^2+h^2}} \mathrm{d}x\mathrm{d}y \ , \qquad (14) \\ R_2 &= \iint_{K_i} \frac{-y}{(x^2+y^2+h^2)^{3/2}} \mathrm{d}x\mathrm{d}y \\ &= \iint_{K_i} \frac{\partial}{\partial y} \frac{1}{\sqrt{x^2+y^2+h^2}} \mathrm{d}x\mathrm{d}y \ , \qquad (15) \\ R_3 &= h \iint_{K_i} \frac{1}{(x^2+y^2+h^2)^{3/2}} \mathrm{d}x\mathrm{d}y \ . \qquad (16) \end{aligned}$$

Once these integrals are computed, the reciprocal mapping is used to get the vector $\overrightarrow{R}$ in the original coordinate system.

When using a parametrisation of the triangle K_i, the first two integrals can be expressed by considering the primitive

$$\begin{aligned} F(a,b,u) &= \int \frac{1}{\sqrt{(a^2+1)u^2+2abu+b^2+h^2}}\ \mathrm{d}u \\ &= \frac{1}{\sqrt{a^2+1}} ln\Big\{ \sqrt{(a^2+1)u^2+2abu+b^2+h^2} \\ &\quad + \sqrt{a^2+1}\ u + \frac{ab}{\sqrt{a^2+1}} \Big\}. \qquad (17) \end{aligned}$$

Then introducing the parameters

$$\lambda_1 = \frac{x_j}{y_j} \ , \ \lambda_2 = \frac{x_j - x_i}{y_j} \ , \ \lambda_3 = -\frac{x_i y_j}{x_j - x_i} \ , \qquad (18)$$

we get

$$\begin{aligned} R_1 &= F(\lambda_2, x_i, y_j) - F(\lambda_2, x_i, 0) - F(\lambda_1, 0, y_j) \\ &\quad + F(\lambda_1, 0, 0) \ , \qquad (19) \\ R_2 &= F(\tfrac{1}{\lambda_1}, 0, x_j) - F(\tfrac{1}{\lambda_1}, 0, 0) + F(0,0,0) \\ &\quad + F(\tfrac{1}{\lambda_2}, \lambda_3, x_i) - F(\tfrac{1}{\lambda_2}, \lambda_3, x_j) - F(0,0,x_i) \ . \qquad (20) \end{aligned}$$

The third integral is much more complicated to handle and the method used depends on the shape of the triangle. We refer to [9], page 81, for a description of the method. We integrate once in x (16) and get

$$R_3 = G(\lambda_2, x_i) - G(\lambda_1, 0) \ , \qquad (21)$$

where

$$G(a,b) = h \int_0^{y_j} \frac{(ay+b)\ dy}{(y^2+h^2)\sqrt{y^2a^2+y^2+2\,aby+b^2+h^2}} \ . \qquad (22)$$

In order to express the algebraic form of G, we introduce the function

$$Atg(t) = Artan\Big(\frac{\sqrt{b^2+h^2a^2}\ t}{|h| \sqrt{t^2 + \frac{a^2(b^2+h^2+h^2a^2)}{b^2}}} \Big) \ . \qquad (23)$$

Let $t_j = \dfrac{a(h^2a - by_j)}{b(ay_j+b)}$ and $t_0 = \dfrac{a^2h^2}{b^2}$.

Depending on the parameters a and b corresponding to the shape of the triangle, we distinguish six cases.

If $ab \neq 0$ we have

- Case 1: $a > 0$,

$$G(a,b) = -\frac{h}{|h|}\big(Atg(t_j) - Atg(t_0)\big). \qquad (24)$$

- Case 2: $a < 0$ and $y_j < -\dfrac{b}{a}$,

$$G(a,b) = \frac{h}{|h|}\big(Atg(t_j) - Atg(t_0)\big). \qquad (25)$$

- Case 3: $a < 0$ and $y_j > -\dfrac{b}{a}$,

$$G(a,b) = -\frac{h}{|h|}\big(Atg(t_j) + Atg(t_0)\big). \qquad (26)$$

If $ab = 0$ we have

- Case 4: $a = 0$ and $b \neq 0$,

$$G(a,b) = \frac{h}{|h|} Arctan\Big(\frac{by_j}{|h|\sqrt{y_j^2+h^2+b^2}}\Big). \qquad (27)$$

- Case 5: $a \neq 0$ and $b = 0$,

$$G(a,b) = \frac{ah}{|ah|}\Big(Arctan\Big(\sqrt{\frac{(a^2+1)y_j^2+h^2}{a^2h^2}}\Big) - Arctan\Big(\frac{1}{|a|}\Big)\Big). \qquad (28)$$

- Case 6: $a = 0$ and $b = 0$,

$$G(a,b) = 0. \qquad (29)$$

The above analytical expressions have been validated by comparing the obtained values to results computed by using quadrature rule. We want to point out that if the domain Ω is a polyhedron then $\overrightarrow{B}$ is evaluated exactly. Moreover the accuracy does not depend on the size of the triangle.

D. Integration over curved triangles

When a part of the boundary is curved, an approximation with flat triangles may not lead to the required accuracy. The use of curved triangles imply the computation of the second sum in (11), denoted S_2. Analytical expressions cannot be obtained anymore.

To numerically evaluate S_2 we first approximate the curved triangle K by a quadratic curved triangle $\tilde{K}$. Then we use a quadrature rule over $\tilde{K}$.

$$\iint_K \overrightarrow{M} \cdot \frac{\overrightarrow{r}(P,Q)}{r^3(P,Q)}\, \overrightarrow{n}(Q)\, \mathrm{d}s(Q) \approx \iint_{\tilde{K}} \overrightarrow{M} \cdot \frac{\overrightarrow{r}(P,Q)}{r^3(P,Q)}\, \overrightarrow{n}(Q)\, \mathrm{d}s(Q)$$

$$\approx \sum_{j=1}^{k} \omega_j\ \overrightarrow{M} \cdot \frac{\overrightarrow{r}(P,\rho_j)}{r^3(P,\rho_j)}\ \overrightarrow{n}(\rho_j)\ , \qquad (30)$$

where ω_j and ρ_j , $j = 1 \cdots k$, are the quadrature weights and nodes which are tabulated.

We point out that the computation of S_2 by a quadrature method is hampered by the quasi-singular behavior of the function $\overrightarrow{M} \cdot \overrightarrow{r}/r^3$ when the point P is close to a triangle K. In this case we give a particular attention to the way the integral over K is evaluated. We use a technique described in [10] that consists in subdividing the integration region $\tilde{K}$ and then use the quadrature rule over each subdivision. We decide on the number of needed subdivisions by evaluating the distance from P to K.

III. Simulated artifacts

The computing method of the magnetic field disturbance described above is linked to artifact reconstruction models [3] to get simulated images of the artifacts. We present a numerically computed artifact due to a titanium cylinder that could represent part of a catheter used in surgery. The experimental image was obtained using a spin-echo sequence along with the two dimensional Fourier transform as described in the introduction. The selection gradient intensity is $10^{-2}\ T.m^{-1}$. The magnetic field $\overrightarrow{B_0}$ $(0.5\ T)$ is aligned along the cylinder axis. The slice imaged is transverse and is located at half height.

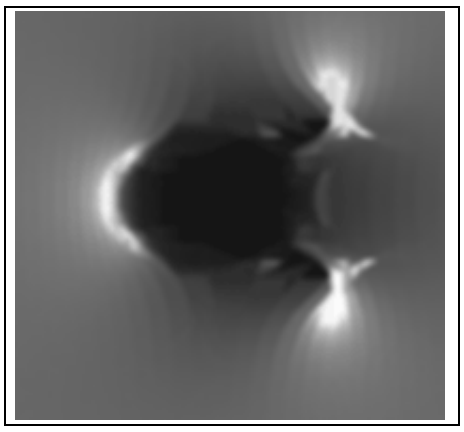

Fig. 2. Numerically computed artifact due to a cylinder.

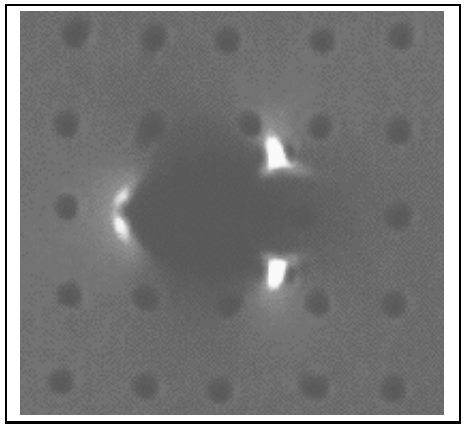

Fig. 3. Experimental image coresponding to Fig. 2.

IV. Conclusion

An analytical technique has been successfully applied for computing the magnetic field induced by a paramagnetic polyhedric body. Since appropriate analytical integrals over curved surfaces are generally not known, this method is somewhat restrictive. We needed to resort to quadrature methods to overcome this limitation.

The advantages of the presented approach is its simplicity and its computational efficiency. This is of great importance since the results are to be linked to the image reconstruction procedure to get simulated figures of susceptibility artifacts in M.R.I.

References

[1] P. G. Morris, ed., *Nuclear Magnetic Resonance in medecine and biology.* Oxford: Clarendon Press, 1986.

[2] K. M. Ludeke , P. Roshmann and R. Tischler, "Susceptibility artifacts in nmr imaging," *Magn. Reson. Imaging*, vol. 3, p. 329, 1985.

[3] S. Beaumont, *Les artefacts de champ magnétique en Imagerie par Résonance Magnétique.* PhD thesis, Thèse de l'Université P. Sabatier, Toulouse, France, 1993.

[4] S. Balac, S. Beaumont, G. Caloz, G. Cathelineau, J. D. De Certaines and J. Lecerf, "Analyse des artefacts liés à la susceptibilité magnétique de biomatériaux en i.r.m.," *I.T.B.M.*, vol. 15, no. 5, 1994.

[5] A. Erricsson, A. Hemmingsson, B. Jung and G. O. Sperber, "Calculation of mri artefacts caused by static field disturbances," *Phys. Med. Biol.*, vol. 33, no. 10, p. 1103, 1988.

[6] S. Posse and W.P. Aue, "Susceptibility artifacts in spin-echo and gradient echo imaging," *J. Magn. Reson.*, vol. 88, p. 473, 1990.

[7] R. Dautray and J. Lions, eds., *Analyse mathématique et calcul numérique pour les sciences et les techniques.* Paris: Masson, 1985.

[8] E. E. Okon and R. F. Harrington, "The potential due to a uniform source distribution over a triangle domain," *Int. J. Num. Meth. in Engng.*, vol. 18, no. 9, p. 1401, 1982.

[9] I. S. Gradshteyn and I. M. Ryzhik, eds., *Table of integrals, series and products.* Academic Press, 1965.

[10] K. Atkinson, "User's guide to a boundary element package for solving integral equation on piecewise smooth surface," Reports on computational mathematics 44, Dept of Mathematics, University of Iowa, 1994.